Pravastatin ameliorates placental vascular defects, fetal growth, and cardiac function in a model of glucocorticoid excess

PRAVASTATIN REVERSES PLACENTAL VASCULAR DEFECTS, RESTORES FETAL GROWTH AND NORMALISES CARDIAC FUNCTION IN A MODEL OF GLUCOCORTICOID EXCESS

Caitlin S. Wyrwoll[1], June Noble[2], Adrian Thomson[2], Dijana Tesic[1], Mark R. Miller[2], Eva A. Rog-Zielinska[2,3], Carmel M. Moran[2], Jonathan R. Seckl[2], Karen E. Chapman[2, 1] and Megan C. Holmes[2].

[1]School of Anatomy, Physiology & Human Biology, The University of Western Australia, 35 Stirling Hwy, Crawley, WA 6009, Australia.

[2]University/BHF Centre for Cardiovascular Science, University of Edinburgh, Edinburgh EH16 4TJ, United Kingdom.

[3]Current address: National Heart & Lung Institute, Imperial College London, Middlesex, UB9 6JH, United Kingdom

Corresponding author: Caitlin Wyrwoll, School of Anatomy, Physiology & Human Biology, The University of Western Australia, 35 Stirling Hwy, Crawley, WA 6009, Australia.

Email: caitlin.wyrwoll@uwa.edu.au.

Classification: BIOLOGICAL SCIENCES: Medical Sciences

Keywords: placenta, 11β-HSD2, glucocorticoids, fetal heart

Short title: Pravastatin ameliorates feto-placental dysfunction

ABSTRACT

Feto-placental glucocorticoid overexposure is a significant mechanism underlying fetal growth restriction and the programming of adverse health outcomes in the adult. Placental glucocorticoid inactivation by 11β-hydroxysteroid dehydrogenase type 2 (11β-HSD2) plays a key role. We previously discovered that *Hsd11b2*$^{-/-}$ mice, lacking 11β-HSD2, show marked underdevelopment of the placental vasculature. We now explore the consequences for fetal cardiovascular development and whether or not this is reversible. We studied *Hsd11b2*$^{+/+}$, *Hsd11b2*$^{+/-}$ and *Hsd11b2*$^{-/-}$ littermates from heterozygous (*Hsd11b*$^{+/-}$) matings at embryonic day (E)14.5 and E17.5, where all three genotypes were present to control for maternal effects. Using high-resolution ultrasound umbilical vein blood velocity in *Hsd11b2*$^{-/-}$ fetuses did not undergo the normal gestational increase seen in *Hsd11b2*$^{+/+}$ littermates. Similarly, the resistance index in the umbilical artery did not show the normal gestational decline. Surprisingly, given that 11β-HSD2 absence is predicted to initiate early maturation, the E/A wave ratio was reduced at E17.5 in *Hsd11b2*$^{-/-}$ fetuses, suggesting impaired cardiac function. Pravastatin administration from E6.5, which increases placental VEGFA and thus vascularization, increased placental fetal capillary volume, ameliorated the aberrant umbilical cord velocity, normalized fetal weight and improved the cardiac function of *Hsd11b2*$^{-/-}$ fetuses. This improved cardiac function occurred despite persisting indications of increased glucocorticoid exposure in the *Hsd11b2*$^{-/-}$ fetal heart. Thus, the pravastatin-induced enhancement of fetal capillaries within the placenta and the resultant hemodynamic changes correspond with restored fetal cardiac function. Statins may represent a useful therapeutic approach to intrauterine growth retardation due to placental vascular hypofunction.

SIGNIFICANCE STATEMENT:

Environmental challenges *in utero* perturb fetal growth and alter subsequent adult health outcomes. The role of the placenta is uncertain. We use a genetically modified mouse model of feto-placental glucocorticoid excess which exhibits decreased placental vascularity and fetal growth restriction. We show that this associates with retarded fetal heart development. Strikingly, treatment with pravastatin restores placental vascularity and reverses retarded fetal growth and cardiovascular development. These results highlight the potential of statins to remedy placental vascular insufficiency and enhance fetal outcomes in compromised pregnancy.

INTRODUCTION

Low birth weight is associated with an increased risk of cardiometabolic disorders in adulthood (1). Frequently underlying this association is elevated fetal exposure to 'stress hormones' - glucocorticoids. Endogenous glucocorticoids (cortisol in humans, corticosterone in rodents) are a key signal in late gestation, which alter developmental trajectories of fetal tissues, predominantly from a proliferative to differentiated state, in preparation for extra-uterine life (2). Fetal overexposure to glucocorticoids in humans, primates and rodents is detrimental for placental and fetal growth and development, and 'programs' higher risk of cardiometabolic disease in later life (3-8). Recent data suggest that the detrimental effects of excess glucocorticoids on fetal growth and development result from direct glucocorticoid actions on the placenta as well as on the fetus itself (9, 10).

The fetus and the placenta are maintained in a low glucocorticoid environment by the abundant expression of feto-placental 11β-hydroxysteroid dehydrogenase-2 (11β-HSD2), an enzyme which inactivates the much higher levels of glucocorticoids arriving from the maternal circulation (11, 12). In humans and in animal models, placental 11β-HSD2 expression is reduced in adverse situations including poor maternal nutrition or maternal stress (13-15). Bypass of this protective enzyme, be it through synthetic glucocorticoids which are poor substrates (9, 16), inhibition (by liquorice) or genetic ablation of *Hsd11b2* which encodes 11β-HSD2 (10), reduces placental weight. This is accompanied by reduced fetal capillary volume, surface area density, length and diameter in the placental labyrinth zone. Underlying these placental changes is a striking reduction in placental expression of vascular endothelial growth factor (VEGF)–A (9, 10) a major driver of placental angiogenesis.

Recent evidence suggests that altered placental function, including its haemodynamics, has a direct impact on the development of fetal organs, particularly the heart (17-22). If compromised placental vascular development due to glucocorticoid excess can be rescued, this raises the possibility of a treatment for adverse effects of placental dysfunction upon the fetal heart and circulation. We therefore assessed placental and umbilical blood velocity and heart growth and function in *Hsd11b2*$^{-/-}$ fetuses and then took advantage of the placental VEGF-releasing effects of pravastatin (23) to determine whether it might rescue or ameliorate the effects of fetal glucocorticoid over-exposure.

RESULTS

Hsd11b2$^{-/-}$ fetuses fail to show the normal gestational maturation in umbilical cord blood velocity and fetal heart function.

To evaluate maturational changes in umbilical cord blood velocity and heart function, fetuses of all 3 genotypes from male and female *Hsd11b2*$^{+/-}$ matings underwent ultrasound analyses at E14.5 (maximum of labyrinth zone 11β-HSD2 expression (11, 12) and before fetal adrenal gland steroidogenesis starts (24)), and at E17.5, (as placental 11β-HSD2 falls, around peak fetal plasma glucocorticoid levels, and just prior to birth, typically E18.5 in *Hsd11b2*$^{+/-}$ mice (10)). Umbilical vein blood velocity normally increases over gestation, as exemplified by the 1.4-fold increase between E14.5 and E17.5 in wild type (*Hsd11b2*$^{+/+}$) fetuses (Fig 1A). Although not different from control littermates at E14.5, umbilical vein blood velocity in *Hsd11b2*$^{-/-}$ fetuses did not undergo the normal gestational increase, such that by E17.5 umbilical vein blood velocity was 24% less than wild-type (Fig 1A). Similarly, the normal gestation decline in umbilical artery resistance (Resistance Index; RI=systole/[systole+diastole]), apparent in *Hsd11b2*$^{+/+}$ and *Hsd11b2*$^{+/-}$ fetuses (18% decrease between E14.5 and E17.5) did not occur in *Hsd11b2*$^{-/-}$ fetuses (Fig 1B). Thus, there was an interaction between gestational age and genotype for both umbilical vein blood velocity and RI. Heart function matures between E14.5 and E17.5, and as the fetal heart becomes more compliant, left ventricle (LV) filling becomes more dependent on passive filling (the E wave) and less dependent on LV filling due to active contraction of the atria (the A wave) (25). This clearly occurs in both *Hsd11b2*$^{+/+}$ and *Hsd11b2*$^{+/-}$ fetuses but did not occur in *Hsd11b2*$^{-/-}$ fetal hearts (Fig 1C). In contrast, myocardial performance index, a combined measure of systolic and diastolic function (25), was unaltered by genotype (see Table S1 for myocardial performance index and a breakdown of each of the cardiac components assessed by ultrasound).

These functional changes were not due to altered gross morphology of the heart. Thus at E17.5 there were no differences in overall cardiac volume (*Hsd11b2*$^{+/+}$: 3.9±0.1, *Hsd11b2*$^{+/-}$: 3.8±0.2, *Hsd11b2*$^{-/-}$: 3.4±0.3 mm^3) or number of cardiomyocytes (*Hsd11b2*$^{+/+}$: 4.1±0.3, *Hsd11b2*$^{+/-}$: 4.1±0.2, *Hsd11b2*$^{-/-}$: 3.8±0.1 x10^6). Perhaps analogously, cardiac function is altered in the absence of gross morphological alteration in mice with cardiomyocyte and vascular smooth muscle-specific deletion of the glucocorticoid receptor (GR) (26).

Altered blood velocity in the *Hsd11b2*$^{-/-}$ umbilical cord prompted us to explore whether this could be attributed to altered umbilical cord structure or function. Histology revealed no significant differences between *Hsd11b2*$^{+/+}$ and *Hsd11b2*$^{-/-}$ in luminal area or wall thickness of the umbilical artery or vein (Table S2). Functionally, isolated umbilical arteries from *Hsd11b2*$^{-/-}$mice tended to be more responsive to vasoconstrictors and have lower basal release of endothelium-dependent mediators. With loss of *Hsd11b2* there was no significant alteration in maximal contractile response to high potassium (Fig 2B) while the thromboxane agonist, U46619 reduced maximal contractile response (Fig 2C). The maximal contraction (K_{max}) to

U46619 was significantly lower in vessels from *Hsd11b2*$^{-/-}$ compared to controls (2.41±0.24 mN vs 3.61±0.45 mN, respectively), although the sensitivity to U46619 (EC_{50}) did not differ between genotypes. Basal endothelial function (basal release of nitric oxide and prostacyclin) was explored through contractile response to L-NAME and indomethacin in the presence of an EC_{50} dose of U46619. L-NAME + indomethacin caused a further 25-50% transient contraction of vessels ~ 2 min after addition, returning to baseline with 5 min (Fig 2D). The contractile response was greatest in the umbilical arteries from control fetuses and lowest in arteries from *Hsd11b2*$^{-/-}$ (19±2% vs ±39±7%, $p<0.05$). Acetylcholine, an endothelium-dependent vasodilator, did not relax umbilical arteries (Fig S1). The ability of umbilical arteries to relax to other vasodilators was confirmed by a concentration-dependent relaxation response to the nitric oxide donor drug, sodium nitroprusside (Fig 2E), with no differences in response between genotypes. This pattern of response concurs with the *in vivo* findings. While increased umbilical artery vasoconstriction and reduced endothelium-dependent functions likely contribute to reduced fetal blood supply in 11β-HSD2 null fetuses, the differences between genotypes and magnitude of the changes were modest and other factors are likely also to be involved (ie. vascular resistance).

Gene expression patterns in *Hsd11b2*$^{-/-}$ fetal hearts reflect glucocorticoid overexposure and earlier maturation.

To investigate glucocorticoid exposure and probe mechanism underlying altered cardiac function in *Hsd11b2*$^{-/-}$ fetuses, we measured levels of mRNA encoding glucocorticoid-responsive genes as well as genes important for contractile function. Cardiac expression of *Tsc22d3* (also known as glucocorticoid-induced leucine zipper; GILZ, a mediator of anti-inflammatory and perhaps other glucocorticoid actions) expression exhibited a normal gestational increase (26) in *Hsd11b2*$^{+/+}$ and *Hsd11b2*$^{+/-}$ fetuses (Fig 3A). *Hsd11b2*$^{-/-}$ fetuses (gestational age and genotype interaction,) had elevated levels at E14.5, consistent with higher glucocorticoid exposure in mid-gestation. Expression of *Myh6* (encoding myosin heavy chain-α, MYHCα, the major contractile protein in the adult heart) normally increases between E14.5 and E17.5 (26), as exemplified by the 1.7-fold increase between E14.5 and E17.5 in *Hsd11b2*$^{+/+}$ and *Hsd11b2*$^{+/-}$ fetal hearts (Fig 3B). While this gestational increase was exaggerated in *Hsd11b2*$^{-/-}$ fetuses, *Myh6* mRNA levels reduced (58%) at E14.5 and increased 1.4-fold at E17.5 compared with *Hsd11b2*$^{+/+}$ littermates (Fig 3B). A similar pattern of expression was observed for the *Atp2a2* gene encoding the calcium-handling protein SERCA2a (Fig 3C). The downregulation of both *Myh6* and *SERCA2a* genes at E14.5 appears at variance with higher glucocorticoid exposure of *Hsd11b2*$^{-/-}$ fetuses, predicted to cause early cardiac maturation. This raises the possibilities that either premature glucocorticoid exposure fails to mimic the normal maturational effects of glucocorticoids upon the heart, or that indirect dysmaturational effects

predominate. Secretion of cardiac natriuretic peptide A (ANP; encoded by *Nppa*) is stimulated by stretch of the myocardium (27) and is considered a marker of cardiomyocyte hypertrophy (28). Its expression increases with gestation, as apparent in *Hsd11b2*$^{+/+}$ fetuses (1.8 fold between E14.5 and E17.5, Fig 3D). However, neither *Hsd11b2*$^{-/-}$ nor *Hsd11b2*$^{+/-}$ fetuses showed this developmental increase in ANP expression in the heart. This suggests the *Hsd11b2*$^{-/-}$ fetal heart tissue is less compliant, as shown by ultrasound *in vivo*. Thus, overall *Hsd11b2*$^{-/-}$ fetuses show complex, gene-specific patterns of premature, exaggerated or reversed maturation of glucocorticoid-sensitive transcripts in the myocardium.

Pravastatin increases labyrinth zone *Vegfa* expression and fetal capillary volume in all genotypes

To determine if the adverse effects of glucocorticoid overexposure on the placental vasculature can be overcome and whether this might beneficially impact on fetal heart development, we administered (i.p.) either pravastatin or saline from E6.5 onwards with the aim of stimulating placental VEGFA production and thereby enhancing vascularization. Consistent with its reported effects on placental VEGF (23), pravastatin up-regulated expression of labyrinth zone *Vegfa* in all genotypes (Fig 4A). The increase in *Hsd11b2*$^{-/-}$ placentas was greater (genotype x treatment), eliminating the genotype difference in placental *Vegfa* expression. Despite its role in regulating *Vegfa* expression (29), labyrinth zone *Pparg* expression levels did not correspond with *Vegfa* patterns (Figure 4B); pravastatin had no effect on *Pparg* mRNA expression and a reduction in *Pparg* mRNA was apparent in both saline and pravastatin-treated *Hsd11b2*$^{-/-}$ placentas.

Corresponding with increased placental *Vegfa*, placental weight increased with pravastatin (Table 1). Stereological assessment of labyrinth zone volume showed that while *Hsd11b2*$^{-/-}$ saline treated placentas appeared smaller this was not statistically significant (Fig 4C). Furthermore, there was only a trend ($p=0.0536$) for labyrinth zone volume increase with pravastatin (Fig 4C). Detailed investigation of fetal capillary volume provided a clearer insight into placental vascular development. Thus, pravastatin modestly increased the volume of fetal capillaries within the labyrinth zone of *Hsd11b2*$^{+/+}$ and *Hsd11b2*$^{+/-}$ fetuses (Fig 4D) but completely rescued the deficit in *Hsd11b2*$^{-/-}$ placentas, with a significant interaction between treatment and genotype. There were no effects of pravastatin on maternal body weight, organ weight or litter size (Table S3).

Pravastatin strikingly attenuates fetal growth restriction and reverses adverse umbilical flow and cardiac function in the *Hsd11b2*$^{-/-}$ placenta and fetus.

In saline-treated pregnancies, *Hsd11b2*$^{-/-}$ fetuses were lighter than littermate controls as previously reported (10) (Table 1). Pravastatin treatment increased fetal weight across all genotypes, though *Hsd11b2*$^{-/-}$ remained lighter than their *Hsd11b2*$^{+/+}$ and *Hsd11b2*$^{+/-}$ littermates (Table 1). However, pravastatin ameliorated the growth retardation in *Hsd11b2*$^{-/-}$ fetuses such that they were the same weight as *Hsd11b2*$^{+/+}$ controls.

Pravastatin had a marked effect on placental blood velocity and fetal heart measures. Overall, pravastatin increased umbilical vein blood velocity (Fig 5A), decreased umbilical artery resistance index (Fig 5B) and increased fetal cardiac E/A wave ratio (Fig 5C) in all genotypes. Notably, pravastatin 'normalised' the aberrant phenotype of *Hsd11b2*$^{-/-}$ fetuses such that there were no genotype differences in umbilical vein blood velocity or fetal cardiac E/A ratio in *Hsd11b2*$^{-/-}$ fetuses from pravastatin-treated dams (Fig 5A and C). In contrast, the resistance index remained increased in both saline-treated and pravastatin-treated *Hsd11b2*$^{-/-}$ fetuses albeit to a lesser extent in the pravastatin-treated *Hsd11b2*$^{-/-}$ fetuses compared to saline treated (Fig 5B).

The effects of pravastatin on cardiac functional changes were not accompanied by gross morphological changes. Thus, there were no differences in overall cardiac volume, ventricular lumen volume or the ratio of ventricular wall thickness to lumen volume (Table S5).

Pravastatin markedly alters fetal cardiac *Ace* and some collagen mRNAs

Expression of glucocorticoid-responsive *Tsc22d3* mRNA was not altered by pravastatin (Fig 6A), consistent with increased glucocorticoid exposure and reflecting similar findings from the initial untreated cohort at E17.5 (Fig 3A). Therefore, the alterations in *Hsd11b2*$^{-/-}$ fetal heart function are likely independent of direct cardiac glucocorticoid action. Similarly, expression of *Mhyc6* and *Atp2a2* were unaffected by pravastatin in all genotypes (Fig 6B and C). While there was no effect of pravastatin on cardiac *Nppa* expression in *Hsd11b2*$^{+/+}$ fetuses (Fig 6D), it increased in pravastatin-treated *Hsd11b2*$^{-/-}$ and *Hsd11b2*$^{+/-}$ fetuses. Thus, pravastatin- rescued cardiac *Nppa* expression in *Hsd11b2*$^{+/-}$ and partially rescued *Hsd11b2*$^{-/-}$ fetuses. Expression of *Ace* was decreased in fetal hearts of all genotypes with pravastatin (Fig 6E) abolishing the genotype difference seen in saline-treated fetuses.

Collagen is a key contributor to cardiac wall stiffness. In fetuses from saline-treated dams, there was an increase in the cardiac expression of *Col1a1* (which determines rigidity (30)) in *Hsd11b2*$^{-/-}$ and *Hsd11b2*$^{+/-}$ fetuses, compared to *Hsd11b2*$^{+/+}$ littermates (Fig 6F). This difference was not evident in fetuses from pravastatin-treated dams. *Col3a1* (which determines elasticity (30) showed a reciprocal effect; *Col3a1* mRNA levels were reduced in hearts of saline-treated *Hsd11b2*$^{-/-}$ and *Hsd11b2*$^{+/-}$ fetuses compared to wild-type littermates (Fig 6G).

However, whilst pravastatin had no effect in *Hsd11b2*$^{+/+}$, it increased *Col3a1* mRNA levels in *Hsd11b2*$^{-/-}$ and *Hsd11b2*$^{+/-}$ fetuses. These expression patterns correspond with the changes in cardiac function. For *Col4a1* (Figure 6H) there was no effect of genotype or treatment, but a significant interaction. Thus, pravastatin increased *Col4a1* expression in hearts of *Hsd11b2*$^{+/+}$ fetuses by 8.5-fold, but decreased it in *Hsd11b2*$^{-/-}$ fetuses (68% decrease). Pravastatin did not alter *Vegfa* and *Pparg* in the fetal heart. These data demonstrate that while pravastatin does not reverse cardiac glucocorticoid overexposure in *Hsd11b2*$^{-/-}$ fetuses, it does change key collagens and other endocrine genes in a pattern which corresponds with enhancement of *Hsd11b2*$^{-/-}$ fetal heart function.

DISCUSSION

Pravastatin treatment dramatically ameliorates the adverse phenotype of *Hsd11b2*$^{-/-}$ fetuses; placental labyrinth zone morphology, umbilical blood velocity, fetal weight and fetal heart function and gene expression are, for the most part, normalised. Thus, despite persistently increased placental and fetal glucocorticoid exposure in *Hsd11b2*$^{-/-}$ fetuses it is possible to counter these adverse outcomes, including the "intra-uterine growth restriction" (IUGR) phenotype. These findings highlight the crucial role of the placenta in informing fetal development and suggest statins as a potential therapy for IUGR with placental vascular insufficiency.

Despite the 'maturational' effects of antenatal glucocorticoids we surprisingly found that *Hsd11b2*$^{-/-}$ fetuses exhibit delayed or impaired cardiac functional maturation. Whether these changes in fetal heart function alter cardiac function in adulthood will be important to uncover in the future, though in this experimental model adult heart function is likely to be influenced by the effect of life-long absence of 11β-HSD2 upon salt regulation, blood pressure and renal function (31), confounding interpretation. Pravastatin treatment then eradicated the impaired *Hsd11b2*$^{-/-}$ fetal cardiac maturation in conjunction with normalizing placental vascular parameters. We postulate that placental and umbilical cord haemodynamics could be an important factor directly influencing fetal heart development. Intervention is required to demonstrate this. However, recent evidence supports the view that the placenta directly influences the development of specific fetal organs, notably the heart. Thus, human placental size and shape are epidemiologically associated with the incidence of cardiovascular disease in later life (17, 32, 33). Thornburg et al. proposed (34) that because the fetal heart beats directly against the resistance of the placental bed, changes in placental blood velocity must impact on fetal heart development. Placental insufficiency (albeit severe – with absent or reversed diastolic velocity in the umbilical artery) results in increased loading of the right ventricle (19). Importantly, extensive work in genetically modified mouse models has revealed the necessity

of a functional placenta for optimal heart development; the cardiac defects exhibited in *Pparγ* and *p38α* null embryos are rectified by targeted placental normalisation (21, 22, 35). Furthermore, mice with genetic disruption of HOXA13, which is not expressed in the heart but is an important transcriptional regulator of placental *Tie2* (and thus placental vascular branching) show abnormal placental endothelium which is associated with reduced ventricular wall thickness in the fetal heart (20), presumably occurring secondarily to the placental defect.

Pravastatin, an HMG-CoA reductase inhibitor which reduces cholesterol biosynthesis, is currently contraindicated in pregnancy. This is due to its potential effects in altering NO bioavailability in the fetal circulation, with detrimental consequences for the fetal brain sparing response to acute hypoxia, as may happen intra-partum (38). However, pravastatin in various mouse models of preeclampsia appears to ameliorate preeclamptic pathology (23, 39), and pravastatin is currently the subject of a randomized control trial to ameliorate severe preeclampsia (40). Three biological compartments are exposed to pravastatin in our model: 1) the maternal, although our experimental design controls for alteration in maternal physiology as all fetal genotypes are generated within the one pregnancy, 2) the placental and 3), the fetal. Restoration of vasculogenesis in preeclamptic placentas following pravastatin has been variously attributed to stimulation of placental VEGF release, soluble Flt-1 (sFlt-1; a VEGF receptor), and placental growth factor (39, 41). Here, pravastatin enhanced labyrinth zone *Vegfa* expression in all genotypes. Accordingly, fetal capillary volume, umbilical vein velocity and umbilical resistance index underwent corresponding changes. Pravastatin will doubtless have placental actions beyond *Vegfa*. Indeed in human first trimester placental explants, pravastatin inhibits insulin-like growth factor 1 receptor function with adverse implications for trophoblast differentiation (42). With regard to the fetus, the levels of pravastatin achieved within the fetal circulation in this current study are unknown but earlier studies have demonstrated that transfer of pravastatin in *ex vivo* human placenta does occur albeit to a limited extent (43, 44). However, it is of interest to note that we observed no induction of *Vegfa* expression in *Hsd11b2*$^{-/-}$ fetal heart, suggesting that if pravastatin is eliciting direct effects on the fetus it may be via different pathways. Whilst we cannot discount the potential for direct effects of pravastatin on the fetus, the intriguing possibility is thus raised that the changes in cardiac parameters are primarily *due to effects of pravastatin on enhancing the placental vasculature*, with effects on the fetal heart occurring secondarily.

Further specific investigations are required to dissect this potential placenta-cardiac axis. Placenta-specific removal of *Hsd11b2* and manipulation of VEGFA specifically in the placenta will be useful to determine how placental vasculature impacts on fetal heart development and function. Nevertheless, our findings suggest the intriguing possibility that using extrinsic

316 factors to enhance placental vasculature in compromised pregnancies could have beneficial
317 impact on fetal heart development and in IUGR more generally. Indeed, other gestational
318 insults, such as fetal hypoxia, which also cause IUGR and cardiovascular programming can be
319 overcome by administration of vitamin C (36, 37). However, the mechanism is likely different;
320 while oxidative stress was attenuated by vitamin C, placental labyrinth zone volume remained
321 unaltered (36, 37).
322
323 Overall, these data add to the growing body of evidence that placental vasculature has a key
324 role in fetal development and programming outcomes. Moreover, enhancement of placental
325 vasculature in compromised pregnancies may be beneficial for fetal heart development and in
326 IUGR.
327
328
329 **METHODS**
330 **Animals**
331 Male and female *Hsd11b2*$^{+/-}$ mice, congenic on the C57BL/6J background (45), were mated
332 overnight and the morning of the day the vaginal plug was identified was designated E0.5. The
333 resultant pregnancies were only analysed if each of the possible offspring genotypes was
334 represented in the litter: *Hsd11b2*$^{+/+}$ ("control" littermates), *Hsd11b2*$^{+/-}$ and *Hsd11b2*$^{-/-}$. This
335 approach controls for alteration in maternal physiology as all fetal genotypes are generated
336 within the one pregnancy. Animals were given standard chow, water and housing arrangements
337 and all studies were conducted in the strictest standards of humane animal care under the
338 auspices of the UK Home Office Animals (Scientific Procedures) Act, 1986 and local ethical
339 committee approval.
340
341 Two groups of dams were utilized for this study. Group 1 underwent characterization of
342 changes in placental and umbilical blood velocity and fetal heart development over gestation.
343 A subset of Group 1 dams underwent ultrasound analyses at E14.5 or E17.5 (n = 8 at each time-
344 point). Following imaging, the pregnant dam was euthanized *in situ*, and scanned fetuses
345 excised following identification by corroboration of position with the ultrasound images.
346 Fetuses were fixed and umbilical cords were collected for subsequent myography studies.
347 Placental and fetal tissues were collected from a further subset of dams (n = 8 at each timepoint)
348 for gene expression analysis.
349
350 Group 2 were injected with either saline (Sal) or 20 μg/kg of pravastatin sodium salt (Prav;
351 Cayman Chemical, Cambridge, UK) i.p. daily from E6.5 onwards. At E17.5, a subset

underwent ultrasound analyses and placentas were collected for stereological analysis (n = 8) whilst an additional cohort (n = 6 – 8) was generated for placental and fetal gene analysis.

Umbilical cords were placed in ice-cold Krebs-Henseleit solution prior to subsequent myography studies. For RNA extractions, placentas were dissected rapidly over wet ice and separated into junctional and labyrinth zones before freezing on dry ice. Fetal hearts were dissected and immediately frozen on dry ice. For histological investigations, whole placentas, umbilical cords and fetuses were fixed in formalin and paraffin embedded. Fetal tails were collected in all cases for genotyping and gendertyping by PCR as described (10). However sex was not taken into account in the final analyses due to an insufficient number of each sex for each possible genotype to reach statistical power.

High resolution ultrasound analysis

In vivo ultrasound assessment was performed using a Vevo 770 ultrasound biomicroscope (Visualsonics; Toronto, Canada) using a RMV707B 30MHz centre frequency transducer. Pregnant mice were scanned as described (26). Fetal-placental units were imaged over a strict 20 min time period, with a minimum of three units being analysed in each pregnancy. Blood velocity within the umbilical artery, vein and placenta was measured (46). Fetal hearts were visualized in B-mode and Doppler measurements were undertaken to determine the E/A wave ratio and myocardial performance index (MPI) (26). Images were recorded for offline analysis.

Placental and umbilical cord morphology

Placental stereological investigations were conducted as described (10). Umbilical cord morphology was ascertained from four cross-sectional haemotoxylin and eosin stained sections taken from the midline of the umbilical cord, 80 μm apart. The umbilical artery and vein area and perimeter were calculated by manually tracing the outer smooth muscle outline and lumen perimeter using Nikon NIS Elements Imaging Software v4.10. (Nikon Instruments Inc., U.S.A.). All measurements were performed by an observer blind to genotype. Treatment and intra-observer error was less than 5%.

Cardiac morphology

Serial haemotoxylin and eosin stained sections were assessed using Nikon NIS Elements Imaging Software v4.10. (Nikon Instruments Inc., U.S.A.). Cardiac tissue volume and cardiomyocyte number were determined using stereological investigations as described (47). Ventricle wall thickness was assessed by measuring the thickness of the wall at the point perpendicular from the center of the longest axis of the ventricle.

Umbilical vessel myography

The contractile and vasodilator capacity of umbilical vessels was assessed by myography, based on modifications of previously established protocols. Umbilical arteries were carefully dissected, cut into lengths of ~1.5 mm, then mounted on a wire myograph (610M; Danish Myo Technology, Aarhus, Denmark) using 25 μm diameter wire. Vessels were placed at 2 mN pretension, allowed to equilibrate for 30-60 min, before establishing vessel viability with high K^+ physiological saline solution (K^+PSS)+noradrenaline (10 μM). Arteries with a contraction of 1 mN or less were excluded from the analysis). Vessels were contracted with increasing doses of thromboxane mimetic (U46619). EC_{80} concentrations of U46619 were chosen to precontract arteries, before carrying out concentration response curves to the endothelium-dependent vasodilator, acetylcholine (ACh), and the endothelium-independent vasodilator, sodium nitroprusside (SNP). To assess basal endothelial activity, vessels were partially precontracted with EC_{50} U46619, before addition of the eNOS inhibitor, L_{ω}-nitro-L-arginine methyl ester (L-NAME; 200 μM), and the cyclooxygenase (COX) inhibitor, indomethacin (10 μM). The data from force transducers were processed by a MacLab/4e analogue-digital converter and displayed through Chart software, version 3.4.3 (AD Instruments, Sussex, UK).

Quantitative qPCR

Total RNA was extracted from tissue using QIAzol® Lysis reagent (Qiagen Sciences, Victoria, Australia) as per the manufacturer's instructions. Total RNA (1 μg) was reverse transcribed using Mouse Moloney leukemia virus reverse transcriptase (M-MLV) and random primers (Promega, Sydney, Australia). The cDNA was subsequently purified with Ultraclean PCR Cleanup kit (MoBio Laboratories, Inc., Carlsbad, CA).

Specific mRNA levels were measured by quantitative (q)RT-PCR on the Rotorgene 6000 system (Corbett Research, Sydney, Australia) using QuantiTect SYBR Green Mastermix (Qiagen Sciences, Victoria, Australia). Primers for *Vegfa*, peroxisome proliferator-activated receptor gamma (*Pparg*), glucocorticoid-induced leucine zipper (GILZ, for *Tsc22d3*), myosin heavy chain 6 alpha (*Myh6*), sarcoplasmic/endoplasmic reticulum calcium ATPase 2 (*Atp2a2*), natriuretic peptide A (*Nppa*), angiotensin I converting enzyme (*Ace*), collagen, type I, alpha 1 (*Col1a1*), collagen, type III, alpha 1 (*Col3a1*), collagen, type IV, alpha 1 (*Col4a1*) were purchased as Qiagen QuantiTect primers with the exception of the internal standards, *Tbp*, *Ppia* and *Sdha*, which were designed using Primer-BLAST (http://www.ncbi.nlm.nih.gov). Primer pairs for all genes are listed in Table S4. Standard curves were generated through tenfold serial dilution of purified PCR products for each gene with analysis using Rotorgene 6000 Software. All samples were normalized against *Tbp*, *Sdha* and *Ppia* using the GeNorm algorithm (48).

Statistical analysis

All data are expressed as mean ± SEM, with each litter representing n = 1, with no more than 1 representative pup per litter analysed. For fetal and placental weights, n = 14-20. Fetal sex was noted but was not taken into account in analyses, including fetal weight, as statistical power was insufficient for analysis by gender as well as genotype. For ultrasound (n = 8) values were normalized to fetal weight. For heart and umbilical cord morphology and gene expression studies, n = 6–8. Two-way ANOVA followed by Tukey's *post hoc* test or one-way ANOVA followed by Tukey's *post hoc* test were used as appropriate. $p<0.05$ was accepted as statistically significant.

Acknowledgements

The funding sources of this study were Wellcome Trust project grant (WT079009) and EU FP7 collaborative grant Developmental origins of healthy and unhealthy ageing (DORIAN, grant n. 278603) to MCH and JRS, and The Raine Medical Research Priming Grant (CSW). ER-Z was funded by a studentship from the British Heart Foundation.

References

1. Godfrey KM & Barker DJ (2001) Fetal programming and adult health. *Public health nutrition* 4(2B):611-624.
2. Fowden AL & Forhead AJ (2015) Glucocorticoids as regulatory signals during intrauterine development. *Exp Physiol*.
3. Wyrwoll CS, Mark PJ, Mori TA, Puddey IB, & Waddell BJ (2006) Prevention of programmed hyperleptinemia and hypertension by postnatal dietary omega-3 fatty acids. *Endocrinology* 147(1):599-606.
4. Wyrwoll CS, Mark PJ, Mori TA, & Waddell BJ (2008) Developmental programming of adult hyperinsulinemia, increased proinflammatory cytokine production, and altered skeletal muscle expression of SLC2A4 (GLUT4) and uncoupling protein 3. *J Endocrinol* 198(3):571-579.
5. Benediktsson R, Lindsay RS, Noble J, Seckl JR, & Edwards CR (1993) Glucocorticoid exposure in utero: new model for adult hypertension. *Lancet* 341(8841):339-341.
6. Lindsay RS, Lindsay RM, Edwards CR, & Seckl JR (1996) Inhibition of 11-beta-hydroxysteroid dehydrogenase in pregnant rats and the programming of blood pressure in the offspring. *Hypertension* 27(6):1200-1204.
7. Nyirenda MJ, Lindsay RS, Kenyon CJ, Burchell A, & Seckl JR (1998) Glucocorticoid exposure in late gestation permanently programs rat hepatic phosphoenolpyruvate carboxykinase and glucocorticoid receptor expression and causes glucose intolerance in adult offspring. *J Clin Invest* 101(10):2174-2181.
8. O'Regan D, Kenyon CJ, Seckl JR, & Holmes MC (2004) Glucocorticoid exposure in late gestation in the rat permanently programs gender-specific differences in adult cardiovascular and metabolic physiology. *Am J Physiol Endocrinol Metab* 287(5):E863-870.
9. Hewitt DP, Mark PJ, & Waddell BJ (2006) Glucocorticoids prevent the normal increase in placental vascular endothelial growth factor expression and placental vascularity during late pregnancy in the rat. *Endocrinology* 147(12):5568-5574.
10. Wyrwoll CS, Seckl JR, & Holmes MC (2009) Altered placental function of 11beta-hydroxysteroid dehydrogenase 2 knockout mice. *Endocrinology* 150(3):1287-1293.
11. Brown RW, *et al.* (1996) The ontogeny of 11 beta-hydroxysteroid dehydrogenase type 2 and mineralocorticoid receptor gene expression reveal intricate control of glucocorticoid action in development. *Endocrinology* 137(2):794-797.
12. Burton PJ, Smith RE, Krozowski ZS, & Waddell BJ (1996) Zonal distribution of 11 beta-hydroxysteroid dehydrogenase types 1 and 2 messenger ribonucleic acid expression in the rat placenta and decidua during late pregnancy. *Biol Reprod* 55(5):1023-1028.
13. Mairesse J, *et al.* (2007) Maternal stress alters endocrine function of the feto-placental unit in rats. *Am J Physiol Endocrinol Metab* 292(6):E1526-1533.
14. O'Donnell KJ, *et al.* (2012) Maternal prenatal anxiety and downregulation of placental 11beta-HSD2. *Psychoneuroendocrinology* 37(6):818-826.
15. Cottrell EC, Seckl JR, Holmes MC, & Wyrwoll CS (2013) Foetal and placental 11beta-HSD2: a hub for developmental programming. *Acta Physiol (Oxf)*.
16. Vaughan OR, Sferruzzi-Perri AN, Coan PM, & Fowden AL (2013) Adaptations in placental phenotype depend on route and timing of maternal dexamethasone administration in mice. *Biol Reprod* 89(4):80.
17. Barker DJ, *et al.* (2012) The placental origins of sudden cardiac death. *Int J Epidemiol* 41(5):1394-1399.
18. Thornburg KL, O'Tierney PF, & Louey S (2010) Review: The placenta is a programming agent for cardiovascular disease. *Placenta* 31 Suppl:S54-59.
19. Kiserud T, Ebbing C, Kessler J, & Rasmussen S (2006) Fetal cardiac output, distribution to the placenta and impact of placental compromise. *Ultrasound Obstet Gynecol* 28(2):126-136.

20. Shaut CA, Keene DR, Sorensen LK, Li DY, & Stadler HS (2008) HOXA13 Is essential for placental vascular patterning and labyrinth endothelial specification. *PLoS Genet* 4(5):e1000073.
21. Adams RH, *et al.* (2000) Essential role of p38alpha MAP kinase in placental but not embryonic cardiovascular development. *Mol Cell* 6(1):109-116.
22. Barak Y, *et al.* (1999) PPAR gamma is required for placental, cardiac, and adipose tissue development. *Mol Cell* 4(4):585-595.
23. Ahmed A, Singh J, Khan Y, Seshan SV, & Girardi G (2010) A new mouse model to explore therapies for preeclampsia. *PLoS ONE* 5(10):e13663.
24. Michelsohn AM & Anderson DJ (1992) Changes in competence determine the timing of two sequential glucocorticoid effects on sympathoadrenal progenitors. *Neuron* 8(3):589-604.
25. Corrigan N, Brazil DP, & Auliffe FM (2010) High-frequency ultrasound assessment of the murine heart from embryo through to juvenile. *Reprod Sci* 17(2):147-157.
26. Rog-Zielinska EA, *et al.* (2013) Glucocorticoid receptor is required for foetal heart maturation. *Hum Mol Genet* 22(16):3269-3282.
27. Rubattu S & Volpe M (2001) The atrial natriuretic peptide: a changing view. *J Hypertens* 19(11):1923-1931.
28. Lu B, *et al.* (2012) Identification of hypertrophy- and heart failure-associated genes by combining in vitro and in vivo models. *Physiological genomics* 44(8):443-454.
29. Jozkowicz A, Dulak J, Piatkowska E, Placha W, & Dembinska-Kiec A (2000) Ligands of peroxisome proliferator-activated receptor-gamma increase the generation of vascular endothelial growth factor in vascular smooth muscle cells and in macrophages. *Acta biochimica Polonica* 47(4):1147-1157.
30. Bishop JE & Laurent GJ (1995) Collagen turnover and its regulation in the normal and hypertrophying heart. *European heart journal* 16 Suppl C:38-44.
31. Kotelevtsev Y, *et al.* (1999) Hypertension in mice lacking 11beta-hydroxysteroid dehydrogenase type 2. *J Clin Invest* 103(5):683-689.
32. Barker DJ, Thornburg KL, Osmond C, Kajantie E, & Eriksson JG (2010) The surface area of the placenta and hypertension in the offspring in later life. *Int J Dev Biol* 54(2-3):525-530.
33. Eriksson JG, Kajantie E, Thornburg KL, Osmond C, & Barker DJ (2011) Mother's body size and placental size predict coronary heart disease in men. *European heart journal* 32(18):2297-2303.
34. Thornburg KL, O'Tierney PF, & Louey S (2010) The Placenta is a Programming Agent for Cardiovascular Disease. *Placenta* 31:S54-S59.
35. Okada Y, *et al.* (2007) Complementation of placental defects and embryonic lethality by trophoblast-specific lentiviral gene transfer. *Nat Biotechnol* 25(2):233-237.
36. Giussani DA, *et al.* (2012) Developmental programming of cardiovascular dysfunction by prenatal hypoxia and oxidative stress. *PLoS One* 7(2):e31017.
37. Richter HG, *et al.* (2012) Ascorbate prevents placental oxidative stress and enhances birth weight in hypoxic pregnancy in rats. *J Physiol* 590(Pt 6):1377-1387.
38. Kane AD, Herrera EA, Hansell JA, & Giussani DA (2012) Statin treatment depresses the fetal defence to acute hypoxia via increasing nitric oxide bioavailability. *J Physiol* 590(Pt 2):323-334.
39. Kumasawa K, *et al.* (Pravastatin induces placental growth factor (PGF) and ameliorates preeclampsia in a mouse model. *Proc Natl Acad Sci U S A* 108(4):1451-1455.
40. Ramma W & Ahmed A (2014) Therapeutic potential of statins and the induction of heme oxygenase-1 in preeclampsia. *Journal of reproductive immunology* 101-102:153-160.
41. Saad AF, *et al.* (2014) Effects of pravastatin on angiogenic and placental hypoxic imbalance in a mouse model of preeclampsia. *Reprod Sci* 21(1):138-145.
42. Forbes K, *et al.* (2015) Statins inhibit insulin-like growth factor action in first trimester placenta by altering insulin-like growth factor 1 receptor glycosylation. *Mol Hum Reprod* 21(1):105-114.

551 43. Zarek J, *et al.* (2013) The transfer of pravastatin in the dually perfused human placenta.
552 *Placenta* 34(8):719-721.
553 44. Nanovskaya TN, *et al.* (2013) Transplacental transfer and distribution of pravastatin.
554 *Am J Obstet Gynecol* 209(4):373 e371-375.
555 45. Holmes MC, *et al.* (2006) The mother or the fetus? 11beta-hydroxysteroid
556 dehydrogenase type 2 null mice provide evidence for direct fetal programming of
557 behavior by endogenous glucocorticoids. *J Neurosci* 26(14):3840-3844.
558 46. Mu J & Adamson SL (2006) Developmental changes in hemodynamics of uterine
559 artery, utero- and umbilicoplacental, and vitelline circulations in mouse throughout
560 gestation. *Am J Physiol Heart Circ Physiol* 291(3):H1421-1428.
561 47. Corstius HB, *et al.* (2005) Effect of intrauterine growth restriction on the number of
562 cardiomyocytes in rat hearts. *Pediatr Res* 57(6):796-800.
563 48. Vandesompele J, *et al.* (2002) Accurate normalization of real-time quantitative RT-
564 PCR data by geometric averaging of multiple internal control genes. *Genome biology*
565 3(7):RESEARCH0034.

566
567

Tables

Table 1: E17.5 fetal and placental weights of *Hsd11b2*$^{+/+}$, *Hsd11b2*$^{+/-}$ and *Hsd11b2*$^{-/-}$ fetuses from saline (Sal) or pravastatin-treated (Prav) dams.

	Sal (n=28)			Prav (n=32)		
	+/+	+/-	-/-	+/+	+/-	-/-
Fetal weight (g)	0.81±0.02[a]	0.83±0.021[ab]	0.73±0.03[c]	0.87±0.01[d]	0.85±0.01[bd]	0.81±0.01[a]
Placental weight (g)	0.09±0.03[a]	0.09±0.02[a]	0.08±0.03[a]	0.1±0.03[b]	0.1±0.03[b]	0.1±0.04[b]

Values are the mean ± SEM. Values without common notation differ significantly ($p<0.05$, two-way ANOVA, Tukey's *post hoc* test). Sal, Saline-treated dams; Prav, Pravastatin-treated dams.

Figure Legends

Figure 1: Umbilical vein velocity (A), umbilical artery resistance index (B) and fetal cardiac E/A wave ratio (C) in *Hsd11b2*$^{+/+}$, *Hsd11b2*$^{+/-}$ and *Hsd11b2*$^{-/-}$ fetuses at E14.5 and E17.5. Values were normalized for fetal weight and are the mean ± SEM (n = 8 per group). Columns without common notation differ significantly ($p<0.05$, two-way ANOVA, Tukey's *post hoc* test).

Figure 2: Contractile and vasodilator function of umbilical arteries. (A) H&E stained cross-section of the umbilical cord. Scale bar = 100 μm. Inset, higher magnification of the umbilical artery used for myography studies. Arrows indicate the presence of endothelial cell nuclei on the lumenal surface of the artery. (B) Maximal contraction of arteries to high potassium physiological saline solution containing noradrenaline (K^+PSS+NA) in animal with disrupted *Hsd11b2* alleles. (C) Maximum vasodilator response to the thromboxane mimetic U46619 in umbilical arteries from *Hsd11b2*$^{-/-}$ fetuses (*$P<0.05$, unpaired t-test of K_{max}). (D) Contractile response to inhibition of basal endothelium-dependent relaxation in response to L_{ω}-nitro-L-arginine methyl ester (L-NAME) and indomethacin (**$P<0.01$, unpaired t-test). (E) Vasodilator response to sodium nitroprusside (SNP). For B, C & E, data shown are the mean ± SEM (n=6, 20, 9 for *Hsd11b2*$^{+/+}$, *Hsd11b2*$^{+/-}$. *Hsd11b2*$^{-/-}$, respectively). For D, data shown are the mean ± SEM (n=5, 11, 8 for *Hsd11b2*$^{+/+}$, *Hsd11b2*$^{+/-}$. *Hsd11b2*$^{-/-}$, respectively).

Figure 3: Relative levels of (A) *Tsc22d3*, (B) *Myh6*, (C) *Atp2a2* and (D) *Nppa* mRNA in hearts of *Hsd11b2*$^{+/+}$, *Hsd11b2*$^{+/-}$ and *Hsd11b2*$^{-/-}$ fetuses at E14.5 and E17.5. Values are means ± SEM (n = 6-8 per group). Columns without common notation differ significantly ($p<0.05$, two-way ANOVA, Tukey's *post hoc* test).

Figure 4: Placental gene expression and morphology in control and pravastatin treated *Hsd11b2*$^{+/+}$, *Hsd11b2*$^{+/-}$ and *Hsd11b2*$^{-/-}$ fetuses. (A) Relative labyrinth zone *Vegfa* mRNA expression and (B) *Pparg* mRNA expression, (C) labyrinth zone (LZ) fraction and (D) fetal capillary (FC) volume. Values are the mean ± SEM (n = 6-8 per group). Columns without common notation differ significantly ($p<0.05$, two-way ANOVA, Tukey's *post hoc* test). Sal, Saline-treated; Prav, Pravastatin-treated, LZ, labyrinth zone; FC, fetal capillaries.

Figure 5: Umbilical vein velocity (A), umbilical artery resistance index (B) and fetal cardiac E/A wave ratio (C) in saline and pravastatin treated *Hsd11b2*$^{+/+}$, *Hsd11b2*$^{+/-}$ and *Hsd11b2*$^{-/-}$ fetuses. Values were normalized for fetal weight and are the mean ± SEM (n = 8 per group). Columns without common notation differ significantly ($p<0.05$, two-way ANOVA, Tukey's *post hoc* test). Sal, Saline-treated; Prav, Pravastatin-treated.

Figure 6: Fetal cardiac gene expression in control and pravastatin treated *Hsd11b2*$^{+/+}$, *Hsd11b2*$^{+/-}$ and *Hsd11b2*$^{-/-}$ fetuses. Relative levels of (A) *Tsc22d3*, (B) *Myh6*, (C) *Atp2a2*, (D) *Nppa*, (E) *Ace*, (F) *Col1a1*, (G) *Col3a1* and (H) *Col4a1*. Values are the mean ± SEM (n = 6-8 per group). Columns without common notation differ significantly ($p<0.05$, two-way ANOVA, Tukey's *post hoc* test). In the case of *Col4a1* *$p<0.05$, t-test of corresponding genotype between treatments. Sal, Saline-treated; Prav, Pravastatin-treated.

Figure 1

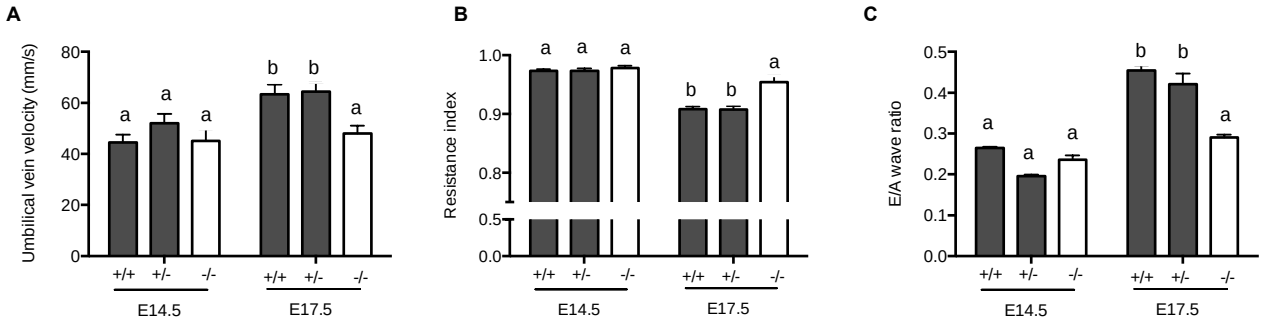
A
Umbilical vein velocity (mm/s)
80
60
40
20
0
a
a
a
b
b
a
+/+ +/- -/- +/+ +/- -/-
E14.5
E17.5
B
Resistance index
1.0
0.9
0.8
0.5
0.0
a
a
a
b
b
a
+/+ +/- -/- +/+ +/- -/-
E14.5
E17.5
C
E/A wave ratio
0.5
0.4
0.3
0.2
0.1
0.0
a
a
a
b
b
a
+/+ +/- -/- +/+ +/- -/-
E14.5
E17.5

631 **Figure 2**

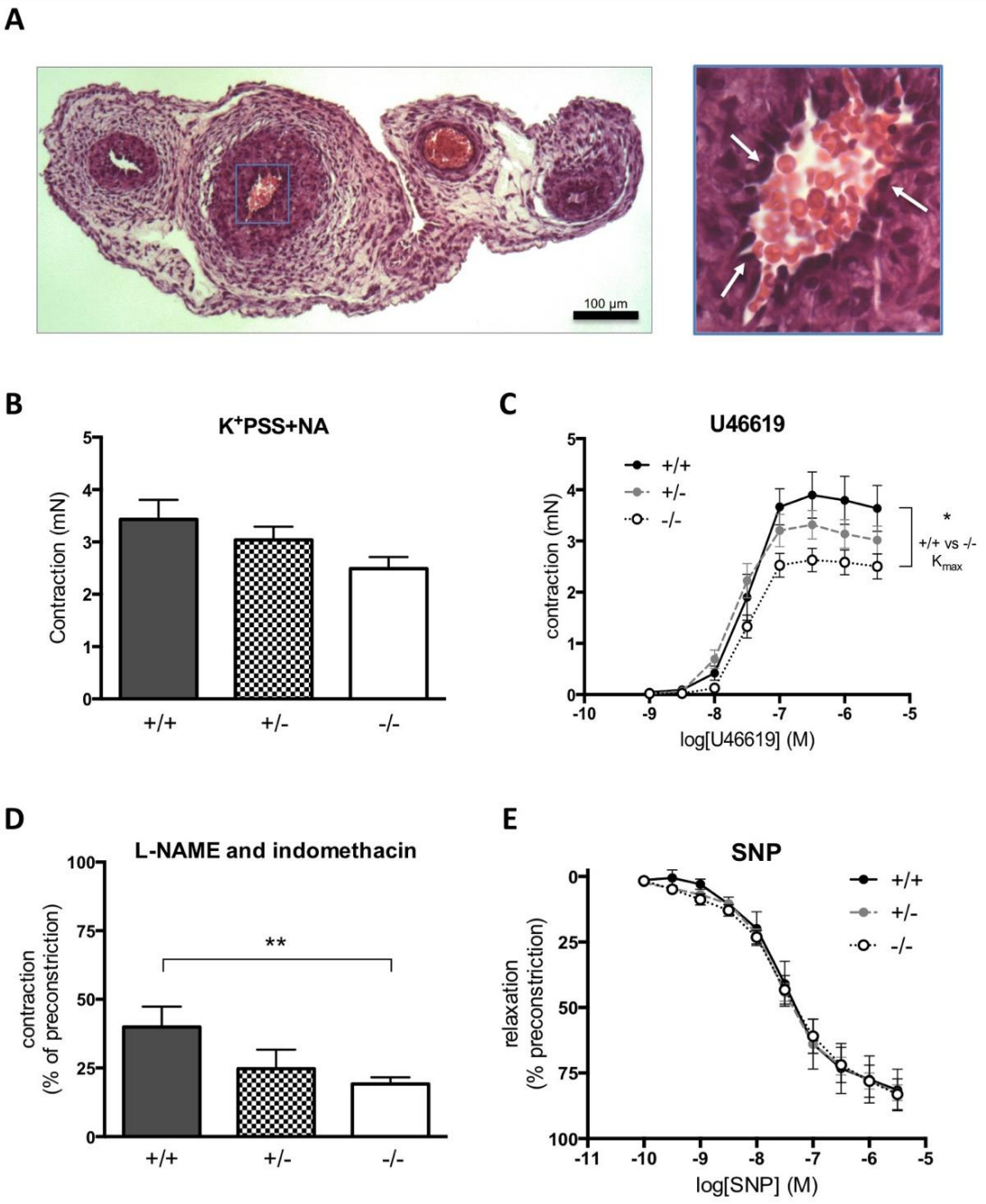

632
633

Figure 3

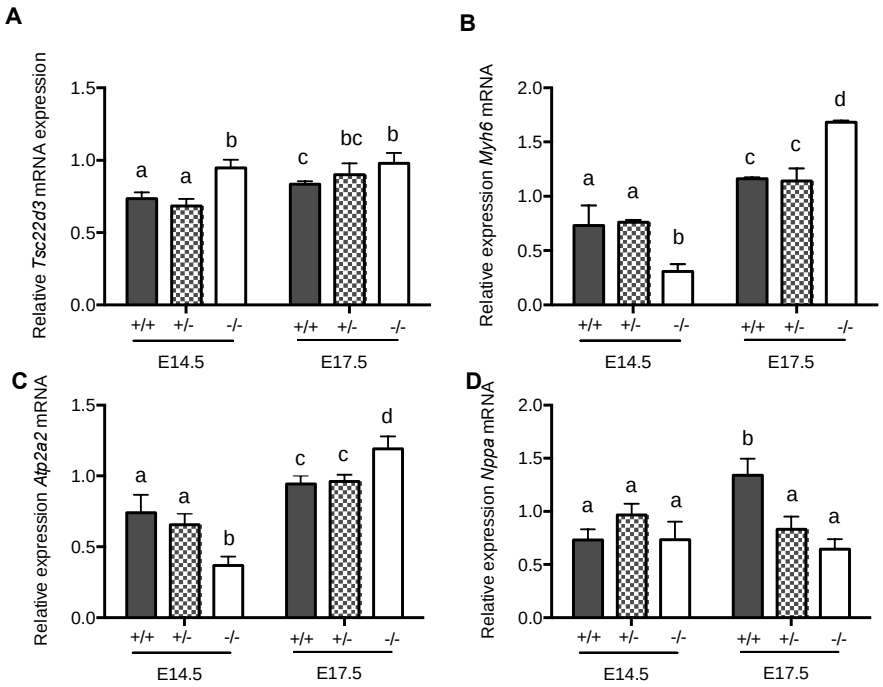
A
Relative Tsc22d3 mRNA expression
1.5
1.0
0.5
0.0
a
a
b
c
bc
b
+/+ +/- -/-
+/+ +/- -/-
E14.5
E17.5
B
Relative expression Myh6 mRNA
2.0
1.5
1.0
0.5
0.0
a
a
b
c
c
d
+/+ +/- -/-
+/+ +/- -/-
E14.5
E17.5
C
Relative expression Atp2a2 mRNA
1.5
1.0
0.5
0.0
a
a
b
c
c
d
+/+ +/- -/-
+/+ +/- -/-
E14.5
E17.5
D
Relative expression Nppa mRNA
2.0
1.5
1.0
0.5
0.0
a
a
a
b
a
a
+/+ +/- -/-
+/+ +/- -/-
E14.5
E17.5

Figure 4

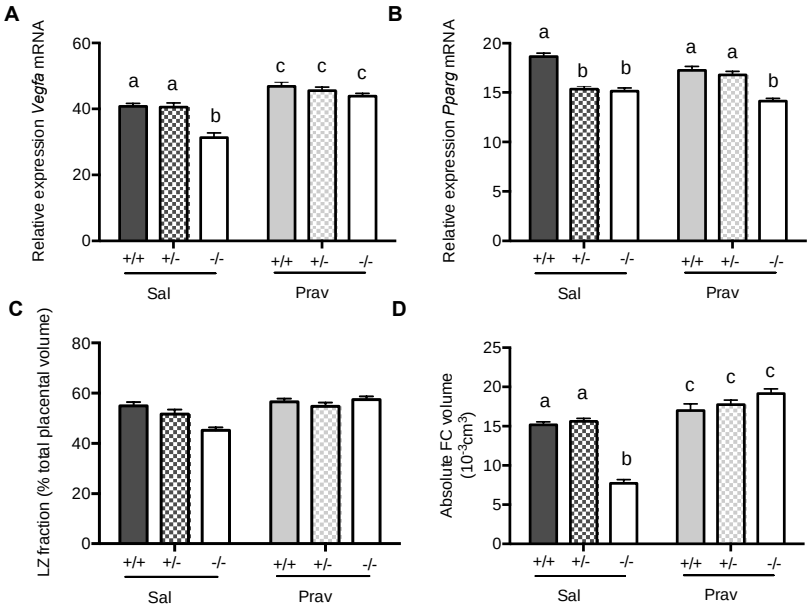
A
Relative expression Vegfa mRNA
60
40
20
0
a a b c c c
+/+ +/- -/- +/+ +/- -/-
Sal
Prav
B
Relative expression Pparg mRNA
20
15
10
5
0
a b b a a b
+/+ +/- -/- +/+ +/- -/-
Sal
Prav
C
LZ fraction (% total placental volume)
80
60
40
20
0
+/+ +/- -/- +/+ +/- -/-
Sal
Prav
D
Absolute FC volume (10-3cm3)
25
20
15
10
5
0
a a b c c c
+/+ +/- -/- +/+ +/- -/-
Sal
Prav

642 **Figure 5**

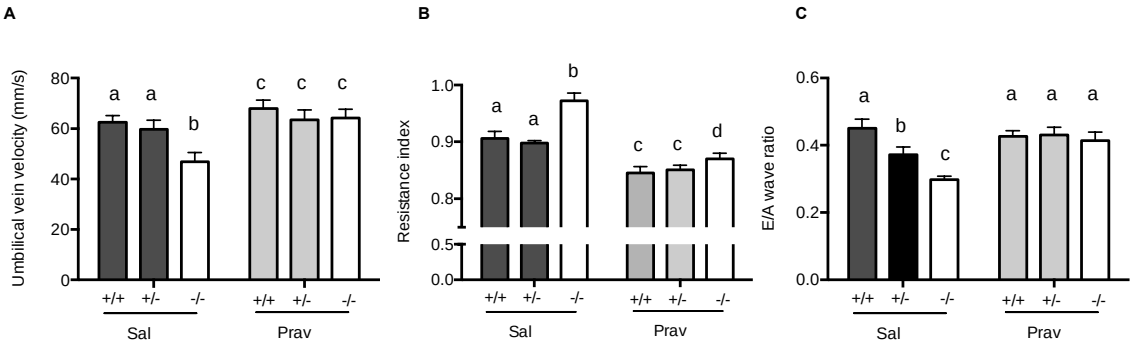

643

644

645

646

Figure 6

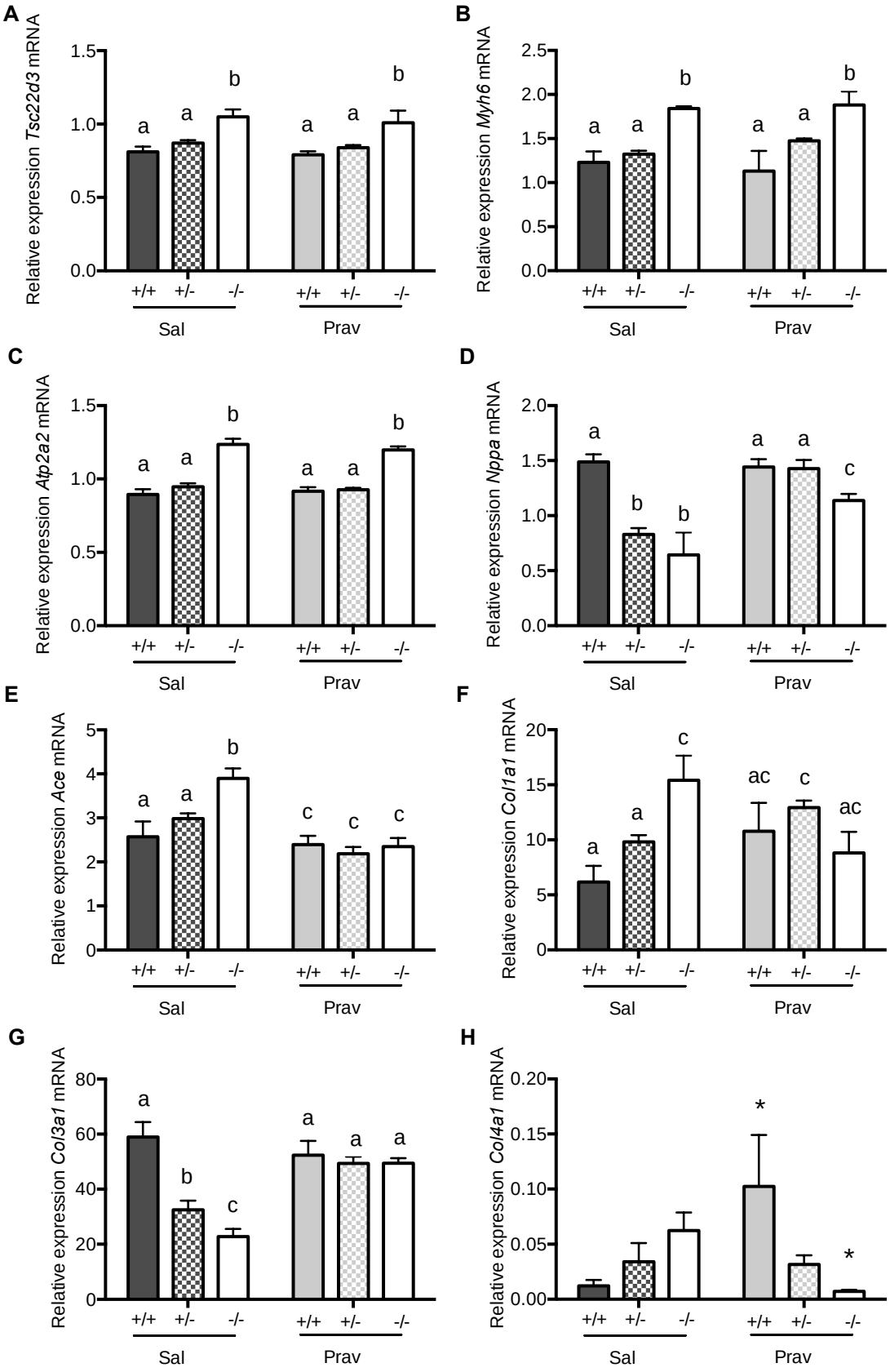
A
Relative expression Tsc22d3 mRNA
B
Relative expression Myh6 mRNA
C
Relative expression Atp2a2 mRNA
D
Relative expression Nppa mRNA
E
Relative expression Ace mRNA
F
Relative expression Col1a1 mRNA
G
Relative expression Col3a1 mRNA
H
Relative expression Col4a1 mRNA
+/+ +/- -/-
Sal
Prav

Supporting Information

Table S1: Myocardial performance index of *Hsd11b2*$^{+/+}$, *Hsd11b2*$^{+/-}$ and *Hsd11b2*$^{-/-}$ fetuses at E14.5 and E17.5. Values without common notation differ significantly.

	E14.5			E17.5		
	Hsd11b2$^{+/+}$	*Hsd11b2*$^{+/-}$	*Hsd11b2*$^{-/-}$	*Hsd11b2*$^{+/+}$	*Hsd11b2*$^{+/-}$	*Hsd11b2*$^{-/-}$
MPI	0.75±0.05^{a}	0.75±0.02^{a}	0.72±0.03^{a}	0.63±0.03^{b}	0.64±0.02^{b}	0.65±0.03^{b}
IVCT (ms)	22±0.3^{a}	23.4±0.1^{a}	22.8±0.2^{a}	18.1±0.2^{b}	16.9±0.4^{b}	19.6±1^{b}
ET (ms)	101.4±5	97.3±3	105.6±5	105.3±2	98.6±5	102.6±4
IVRT (ms)	26.1±3^{a}	24.8±2^{a}	25.9±3^{a}	22.4±3^{b}	20.1±1^{b}	21.7±0.5^{b}
EDD (mm/s^2)	1542±481^{a}	1329±312^{a}	1376±548^{a}	3128±682^{b}	3308±384^{b}	1365±445^{a}
EF (%)	73.8±3.5^{a}	76.2±2^{a}	71.8±1.4^{a}	85.2±2.1^{b}	81.3±1.9^{b}	82.6±1.5^{b}

Values are the mean ± SEM. MPI, myocardiacl performance index; IVCT, isovolumetric contraction time; ET, ejection time; IVRT, isovolumetric relaxation time; EDD, early diastolic deceleration; EF, ejection fraction

Table S2: Lumen and vessel wall area of umbilical arteries and vein from *Hsd11b2*$^{+/+}$ and *Hsd11b2*$^{-/-}$ fetuses.

	Umbilical artery		Umbilical vein	
	Hsd11b2$^{+/+}$	*Hsd11b2*$^{-/-}$	*Hsd11b2*$^{+/+}$	*Hsd11b2*$^{-/-}$
Lumen area (μm^2)	4211±1265	3624±986	36211±8246	29425±6937
Vessel wall area (μm^2)	32646±1324	28436±2534	24328±879	18656±2289

Values are the mean ± SEM

Table S3: Pravastatin treatment does not affect maternal body weight, organ weight or litter size.

	Sal (n=28)	Prav (n=32)
E17.5 maternal weight (g)	31.7±1.7	32.0±1.9
Brain weight (g)	0.46±0.01	0.47±0.01
Liver weight (g)	1.63±0.07	1.8±0.06
Heart weight (g)	0.15±0.01	0.18±0.01
Left kidney weight (g)	0.15±0.01	0.15±0.01
Litter size	8.1±0.8	9.1±0.5

Values are the mean ± SEM. Sal, Saline-treated dams; Prav, Pravastatin-treated dams.

Table S4: PCR conditions

Gene	**Qiagen QuantiTect name or Primer sequence**
Vegfa	QT00160769
Pparg	QT00100296
Tsc22d3	QT01552005
Nr3c1	QT00160349
Nr3c2	QT00312305
Myh6	QT00160902
Atp2a2	QT00149121
Nppa	QT00250922
Ace	QT00100135
Col1a1	QT 00162204
Col3a1	QT 01055516
Col4a1	QT 00287392
Col5a1	QT 01055474
Sdha	F, 5'-TGGGGCGACTCGTGGCTTTC- 3′
	R, 5'-CCCCGCCTGCACCTACAACC- 3′
Ppia	F, 5'-AGCATACAGGTCCTGGCATC- 3′
	R, 5'-TTCACCTTCCCAAAGACCAC- 3′
Tbp	F 5' GGGAGAATCATGGACCAGAA '3 R 5' CCGTAAGGCATCATTGGACT '3

Qiagen QuantiTect primer name and primer sequences for analysis and reference genes. F, forward; R, reverse.

Table S5: Pravastatin treatment does not alter overall cardiac volume, ventricular lumen volume or the ratio of ventricular wall thickness to lumen volume of *Hsd11b2*$^{+/+}$, *Hsd11b2*$^{+/-}$, and *Hsd11b2*$^{-/-}$ fetuses.

	Sal			Prav		
	Hsd11b2$^{+/+}$	*Hsd11b2*$^{+/-}$	*Hsd11b2*$^{-/-}$	*Hsd11b2*$^{+/+}$	*Hsd11b2*$^{+/-}$	*Hsd11b2*$^{-/-}$
Cardiac volume (mm^3)	3.8±0.4	3.6±0.3	3.5±0.2	3.7±0.2	3.8±0.3	3.6±0.2
LV lumen volume (mm^3)	0.87±0.16	0.6±0.08	1.07±0.2	1.15±0.1	0.87±0.07	0.76±0.12
LV wall thickness: Lumen volume	0.46±0.03	0.45±0.02	0.49±0.05	0.44±0.04	0.43±0.05	0.45±0.02
RV lumen volume (mm^3)	0.89±0.06	0.58±0.18	0.88±0.13	1.04±0.2	0.62±0.1	0.79 ±0.1
RV wall thickness: Lumen volume	0.42±0.05	0.39±0.04	0.44±0.06	0.43±0.02	0.41±0.03	0.41±0.04

Values are the mean ± SEM. Sal, Saline-treated; Prav, Pravastatin-treated; LV, left ventricle; RV, right ventricle

Figure S1: Acetylcholine (ACh) did not relax umbilicial arteries. There were no significant differences between genotypes. Symbols shown are mean±SEM (n=6, 12 & 9 for *Hsd11b2*$^{+/+}$, *Hsd11b2*$^{+/-}$, *Hsd11b2*$^{-/-}$, respectively).

Figure S1